Wave Field Synthesis of moving sources with arbitrary trajectory and velocity profile

Gergely Firtha and Peter Fiala
Budapest University of Technologies and Economics, firtha,fiala@hit.bme.hu

(Dated: September 7, 2016)

The sound field synthesis of moving sound sources is of great importance when dynamic virtual sound scenes are to be reconstructed. Previous analytically correct solutions considered only virtual sources moving uniformly along a straight trajectory, synthesized using a linear loudspeaker array. This article presents the synthesis of point sources following an arbitrary trajectory. Under high-frequency assumptions 2.5D Wave Field Synthesis driving functions are derived for arbitrary shaped secondary source contours by adapting the stationary phase approximation to the dynamic description of sources in motion. It is explained, how a referencing function should be chosen in order to optimize the amplitude of synthesis on an arbitrary receiver curve. Finally a finite difference implementation scheme is considered, making the presented approach suitable for real-time applications.

PACS numbers: Valid PACS appear here

I. INTRODUCTION

Wave Field Synthesis (WFS) aims at the physical reproduction of a target sound field within an extended listening area using a densely spaced loudspeaker ensemble, termed as the *secondary source distribution (SSD)*. The loudspeakers are fed with properly derived *driving functions*, so that the field in the listening area—i.e. the resultant field of the secondary sources—coincides with the target sound field. WFS is an implicit solution methodology, where the driving functions are extracted from an appropriate boundary integral representation of the target wave field. Early WFS theory considered planar and linear SSDs, where the driving functions are obtained from the Rayleigh-integral representation of the target field[1–3]. Recently it was shown, that in the high frequency domain WFS can be applied to arbitrarily shaped enclosing secondary arrays[4], utilizing the high frequency approximation of the general Kirchhoff-Helmholtz integral[5]. In an upcoming work from the present authors it is demonstrated, that by introducing a proper *referencing function* WFS is capable of amplitude correct synthesis along an arbitrary listening curve using an arbitrary shaped SSD contour[6].

In addition to the synthesis of stationary virtual sound fields—e.g. plane waves and stationary point sources—the synthesis of moving point sources gained increasing interest. For this dynamic case the primary challenge is the proper reconstruction of the Doppler-shift, which is inherently solved when the dynamic description of the target field is adapted to the WFS theory[7,8]. As a special case, the synthesis of sources under uniform motion using a planar/linear SSD is well-studied. In recent articles by the authors driving functions were obtained for linear secondary sources by adapting traditional WFS theory to the dynamic scenario[9], and by alternatively applying the explicit spectral solution, termed as the Spectral Division Method[10].

It is well known that spatial aliasing artifacts, resulting from the discretization of the SSD, are more significant for moving sources[8,11]. The spectral solution provides a useful tool for the quantitative investigation of spatial aliasing[12]. It was shown that linear secondary arrays yield increased spatial aliasing artifacts, which verifies the necessity of WFS driving functions for non-linear (curved) SSDs.

The present article deals with the general solution of the dynamic SFS problem. By adapting the moving source dynamics to unified WFS formulation[6], driving functions are given for arbitrary shaped SSDs, ensuring amplitude correct synthesis on an arbitrary shaped receiver curve in the high-frequency region. The paper is structured as follows: Section II.A introduces the concept of wave field synthesis, and Section II.B derives the sound field of a monopole following an arbitrary trajectory. Section III adapts WFS to the field of the moving source, and derives 3D driving functions for arbitrarily shaped surface SSD, as well as 2.5D driving functions for curved SSD contours. By utilizing the referencing function concept, referencing functions are derived for the 2.5D case, allowing amplitude correct synthesis along a predefined reference curve. Section IV presents numerical validation of the derived driving functions. Finally, Section V presents an efficient computation scheme that allows real time computation of the driving functions.

II. THEORETICAL BACKGROUND

A. Wave Field Synthesis theory

The general SFS problem can be formulated as follows. Consider a secondary source distribution consisting of identical sources, located at $\mathbf{x}_0 = [x_0,\ y_0,\ z_0]^{\mathrm{T}} \in S$. The synthesized pressure field at the receiver position $\mathbf{x}$ reads

$$p(\mathbf{x},t) = \int_S \int_{-\infty}^{\infty} d(\mathbf{x}_0,t_0) h(\mathbf{x}-\mathbf{x}_0, t-t_0) \mathrm{d}t_0 \mathrm{d}\mathbf{x}_0, \quad (1)$$

where $h(\mathbf{x},t)$ is the spatio-temporal impulse response of the secondary sources and $d(\mathbf{x},t)$ is the driving function

to be derived, so that the synthesized sound field equals to the target sound field over an extended area.

Traditional WFS theory constructs the driving functions from the Rayleigh-integral representation of the target sound field: for an infinite planar boundary surface the *Kirchhoff-Helmholtz integral (KHI)*—that represents any source free sound field inside an enclosure as a double layer potential—degenerates to a single layer potential over the Rayleigh-plane, with the integral kernel being the 3D Green's function, describing the field of an acoustic point source. In the aspect of WFS with a planar SSD consisting of a continuous distribution of 3D point sources the Rayleigh-integral implicitly contains the driving functions in the form of the normal derivative of the target field taken on the SSD[3,13].

As it was pointed out by Fazi[5]—emerging from the equivalent scattering interpretation of the general SFS problem—in case of convex enclosing boundaries and high-frequencies (where the wavelength is significantly smaller than the boundary dimensions), the *Kirchoff/Physical Optics approximation* may be applied to the KHI. Under these assumptions the boundary can be considered locally planar, and the KHI is approximated locally by the Rayleigh-integral. The pressure field inside the enclosure is written in the time domain as

$$p(\mathbf{x},t) = \int_S \int_{-\infty}^{\infty} \overbrace{-2w(\mathbf{x}_0)\frac{\partial}{\partial \mathbf{n}_{\text{in}}} p(\mathbf{x}_0,t_0)}^{d_{3\text{D}}(\mathbf{x}_0,t_0)} g(\mathbf{x}-\mathbf{x}_0,t-t_0)\mathrm{d}t_0\mathrm{d}\mathbf{x}_0 \tag{2}$$

and equivalently in the frequency domain (assuming a time dependency $\mathrm{e}^{\mathrm{j}\omega t}$) as

$$P(\mathbf{x},\omega) = \int_S \overbrace{-2w(\mathbf{x}_0)\frac{\partial}{\partial \mathbf{n}_{\text{in}}} P(\mathbf{x}_0,\omega)}^{D_{3\text{D}}(\mathbf{x}_0,\omega)} G(\mathbf{x}-\mathbf{x}_0,\omega)\mathrm{d}\mathbf{x}_0, \tag{3}$$

where $g(\mathbf{x},t) = \frac{1}{4\pi}\frac{\delta(t-|\mathbf{x}|/c)}{|\mathbf{x}|}$ and $G(\mathbf{x},\omega) = \frac{1}{4\pi}\frac{\mathrm{e}^{-\mathrm{j}\omega|\mathbf{x}|/c}}{|\mathbf{x}|}$ are the 3D Green's function in the temporal and frequency domain respectively, with c being the speed of sound. Here

$$\frac{\partial}{\partial \mathbf{n}_{\text{in}}} P(\mathbf{x}_0) = \left\langle \mathbf{n}_{\text{in}}(\mathbf{x}_0)\cdot\nabla P(\mathbf{x})|_{\mathbf{x}=\mathbf{x}_0}\right\rangle$$

denotes the inward normal derivative of the incident field taken on the boundary surface. The integrals implicitly contain the 3D driving functions.

Only those parts of the SSD contribute to the integral, where the field of the secondary element propagates in the same direction as the target sound field. This part of the SSD is often termed as the *illuminated region*, and is selected by the window function $w(\mathbf{x}_0)$:

$$w(\mathbf{x}_0) = \begin{cases} 1 & \langle \mathbf{k}(\mathbf{x}_0)\cdot\mathbf{n}_{\text{in}}(\mathbf{x}_0)\rangle > 0 \\ 0 & \text{elsewhere,} \end{cases} \tag{4}$$

where $\mathbf{k}(\mathbf{x}_0)$ denotes the *local wavenumber* vector of the virtual sound field at the SSD. In the aspect of WFS this type of windowing is referred to as *secondary source criterion*[4,14].

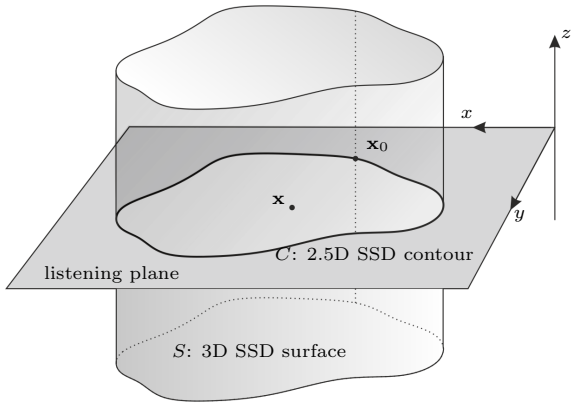

FIG. 1. General 3D WFS geometry for the derivation of 2.5D driving functions. The SSD surface $S = f(x_0, y_0)$ is chosen to be independent of the z-coordinate in order to be able to evaluate the integral with respect to z_0 using the SPA. If the virtual sound field is a 2D one, propagating in the direction parallel to the listening plane the the SSD can be interpreted as a continuous set of infinite vertical line sources along C (described by the 2D Green's function), capable of the perfect synthesis of a virtual 2D field inside the enclosure. ERRE MOST NINCS HIVATKOZS AZ ELS SECTIONBEN!

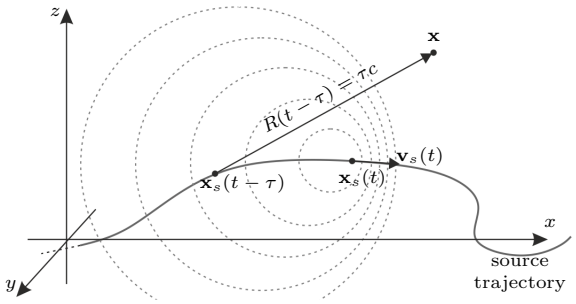

FIG. 2. Arrangement for the description of a source, moving at an arbitrary trajectory

The local wavenumber vector can be defined as

$$\mathbf{k}(\mathbf{x}) = -\nabla\angle P(\mathbf{x},\omega), \tag{5}$$

where $\angle$ denotes the phase of an arbitrary sound field. The wavenumber vector points in the direction of local propagation, and is perpendicular to the wave front.

Note that the derived driving functions would ensure perfect synthesis for a planar SSD, where the enclosed sound field degenerates to a half space. For any other SSD geometries high-frequency assumptions must hold.

B. Description of moving sources on arbitrary 3D trajectory

Consider a translation invariant point source, moving along an arbitrary trajectory $\mathbf{x}_s(t) = [x_s(t),\ y_s(t),\ z_s(t)]^{\mathrm{T}}$ and radiating with the source time history $q(t)$. The radiated field $p_m(\mathbf{x},t)$ at an arbitrary receiver position $\mathbf{x}$ can be written as the convolution of the source signal and the time varying

impulse response of the moving source:

$$p_m(\mathbf{x},t) = \int_{-\infty}^{\infty} q(\hat{t}) g_m(\mathbf{x}-\mathbf{x}_s(\hat{t}), t-\hat{t}) \mathrm{d}\hat{t}, \qquad (6)$$

where the impulse response

$$g_m(\mathbf{x}-\mathbf{x}_s(\hat{t}), t-\hat{t}) = \frac{1}{4\pi} \frac{\delta\left(t-\hat{t}-\frac{|\mathbf{x}-\mathbf{x}_s(\hat{t})|}{c}\right)}{|\mathbf{x}-\mathbf{x}_s(\hat{t})|} \qquad (7)$$

is the *retarded Green's function* and $\hat{t}$ denotes the *emission time*. In order to exploit the sifting property of the Dirac delta in (6), a new variable t' is introduced as $t'(\hat{t}) = \hat{t} + \frac{|\mathbf{x}-\mathbf{x}_s(\hat{t})|}{c}$. The Jacobian reads as

$$\frac{\mathrm{d}t'(\hat{t})}{\mathrm{d}\hat{t}} = 1 - \frac{1}{c} \frac{\left\langle \frac{\partial}{\partial \hat{t}} \mathbf{x}_s(\hat{t}) \cdot (\mathbf{x}-\mathbf{x}_s(\hat{t})) \right\rangle}{|\mathbf{x}-\mathbf{x}_s(\hat{t})|} \qquad (8)$$

where $\mathbf{v}_s(\hat{t}) = \frac{\partial}{\partial \hat{t}} \mathbf{x}_s(\hat{t})$ denotes the source velocity vector. As the Dirac-delta sifts out $t'(\hat{t}) = t$, the radiated field reads as

$$p_m(\mathbf{x},t) = \frac{1}{4\pi} \frac{q\left(t-\frac{|\mathbf{x}-\mathbf{x}_s(\hat{t})|}{c}\right)}{|\mathbf{x}-\mathbf{x}_s(\hat{t})| - \frac{1}{c}\left\langle \mathbf{v}_s(\hat{t}) \cdot (\mathbf{x}-\mathbf{x}_s(\hat{t})) \right\rangle}, \qquad (9)$$

where $\hat{t}$ satisfies

$$t - \hat{t} = \frac{|\mathbf{x}-\mathbf{x}_s(\hat{t})|}{c}. \qquad (10)$$

Conventionally the radiated field is expressed in terms of the propagation time-delay $\tau(\mathbf{x},t) = t - \hat{t}$. Introducing $\Delta(\mathbf{x},t)$ for the attenuation factor the radiated field is given as

$$p_m(\mathbf{x},t) = \frac{1}{4\pi} \frac{q(t-\tau(\mathbf{x},t))}{\Delta(\mathbf{x},t-\tau)}, \qquad (11)$$

with

$$\Delta(\mathbf{x},t) = |\mathbf{x}-\mathbf{x}_s(t)| - \left\langle \frac{1}{c} \mathbf{v}_s(t) \cdot (\mathbf{x}-\mathbf{x}_s(t)) \right\rangle = \\ = R(\mathbf{x},t)\,(1 - M(t)\cos\vartheta(\mathbf{x},t)) \qquad (12)$$

where $R(\mathbf{x},t)$ is the source-receiver distance, $M(t) = |\mathbf{v}_s(t)|/c$ is the Mach-number, $\vartheta(\mathbf{x},t)$ is the angle between the velocity vector and the source-receiver vector, and equation

$$R(\mathbf{x},t-\tau) - c\tau = |\mathbf{x}-\mathbf{x}_s(t-\tau)| - c\tau = 0 \qquad (13)$$

is satisfied. In equation (12) $(1 - M(t)\cos\vartheta(\mathbf{x},t))^{-1}$ is termed as the *Doppler-factor*, describing the relative frequency-shift in case of a harmonic source signal[15]. For subsonic velocities (i.e. $v < c$) only the positive root of the quadratic equation ($\tau > 0$) is taken into consideration[16]. Note, that the evaluation of equation (11) requires the solution of the non-linear equation (13) for each time instant and listener position.

III. WFS OF MOVING SOURCES

A. 3D driving functions

The dynamic description obtained in the previous section can be directly used for the synthesis of moving sources. For the sake of simplicity assume a harmonic source time-history $q(t) = \mathrm{e}^{\mathrm{j}\omega_0 t}$, with the oscillation frequency ω_0. The radiated field reads

$$P_m(\mathbf{x},t,\omega_0) = \frac{1}{4\pi} \frac{\mathrm{e}^{\mathrm{j}\omega_0(t-\tau(\mathbf{x},t))}}{\Delta(\mathbf{x},t-\tau(\mathbf{x},t))}. \qquad (14)$$

The 3D WFS driving functions in the time-frequency domain can be expressed from (2) by evaluating (-2) times the normal derivative of the sound field on the SSD

$$D_{3\mathrm{D}}(\mathbf{x}_0,t,\omega_0) = -2w \left\langle \mathbf{n}_{\mathrm{in}}(\mathbf{x}_0) \cdot \nabla P_m(\mathbf{x},t,\omega_0)|_{\mathbf{x}=\mathbf{x}_0} \right\rangle \qquad (15)$$

The gradient of the sound field is expressed as

$$\nabla P_m(\mathbf{x},t,\omega_0) = \\ -\frac{1}{4\pi}\left(\frac{\nabla\left(\Delta(\mathbf{x},t-\tau)\right)}{\Delta(\mathbf{x},t-\tau)} + \mathrm{j}\omega_0 \nabla\tau(\mathbf{x},t)\right) \frac{\mathrm{e}^{\mathrm{j}\omega_0(t-\tau(\mathbf{x},t))}}{\Delta(\mathbf{x},t-\tau)}, \qquad (16)$$

where $\omega_0\nabla\tau(\mathbf{x},t) = \mathbf{k}(\mathbf{x},t)$ is the local wavenumber vector. For the Physical Optics approximation high-frequency/far-field assumptions are standard prerequisitions. In this case the phase changes rapidly compared to the amplitude ($\mathrm{j}\omega_0\nabla\tau(\mathbf{x},t) \gg \frac{\nabla(\Delta(\mathbf{x},t-\tau))}{\Delta(\mathbf{x},t-\tau)}$) and the gradient can be approximated as

$$\nabla P_m(\mathbf{x},t,\omega_0) \approx -\frac{\mathrm{j}\omega_0\nabla\tau(\mathbf{x},t)}{4\pi} \frac{\mathrm{e}^{\mathrm{j}\omega_0(t-\tau(\mathbf{x},t))}}{\Delta(\mathbf{x},t-\tau)} \qquad (17)$$

$$= -\mathrm{j}\mathbf{k}(\mathbf{x},t) P_m(\mathbf{x},t,\omega_0). \qquad (18)$$

This high-frequency gradient approximation is a local plane wave approximation of the moving source sound field. The approximation can be applied for any harmonic target sound field in the high-frequency region, leading to a general 3D WFS driving function

$$D_{3\mathrm{D}}(\mathbf{x}_0,t,\omega_0) = -2w\,\langle\, \mathbf{k}(\mathbf{x}_0,t) \cdot \mathbf{n}_{\mathrm{in}}(\mathbf{x}_0)\rangle\, P(\mathbf{x}_0,t,\omega_0). \qquad (19)$$

This result is a generalization of the driving functions given in [(20),17]

The gradient of the propagation time delay $\nabla\tau$ can be evaluated by implicit differentiation of (13):

$$\nabla\tau(\mathbf{x},t) = \frac{1}{c} \frac{\mathbf{x}-\mathbf{x}_s(t-\tau)}{\Delta(\mathbf{x},t-\tau)}, \qquad (20)$$

and by denoting the normal component of the source-SSD distance by $R_{\mathrm{n}}(\mathbf{x}_0,t) = \langle(\mathbf{x}_0 - \mathbf{x}_s(t)) \cdot \mathbf{n}_{\mathrm{in}}(\mathbf{x}_0)\rangle$ the driving functions read

$$D_{3\mathrm{D}}(\mathbf{x}_0,t,\omega_0) = w\frac{\mathrm{j}k_0}{2\pi} \frac{R_{\mathrm{n}}(\mathbf{x}_0,t-\tau)}{\Delta(\mathbf{x}_0,t-\tau)} \frac{\mathrm{e}^{\mathrm{j}\omega_0(t-\tau(\mathbf{x}_0,t))}}{\Delta(\mathbf{x}_0,t-\tau)}, \qquad (21)$$

with $k_0 = \omega_0/c$ being the source wavenumber, and the window function $w(\mathbf{x}_0,t)$ given by (4), with the dependencies suppressed for the sake of brevity.

B. 2.5D driving functions

Practical WFS implementations apply an SSD curve instead of a surface, located at the listening plane $\mathbf{x}_0 = [x_0,\ y_0, 0]$. In order to derive the corresponding driving functions, the geometry shown in Figure 1 is used. The listener plane is assumed to be at $z = 0$ (i.e. $\mathbf{x} = [x,\ y,\ 0]^{\mathrm{T}}$), and the trajectory of the virtual source is also restricted to $z_s(t) = 0$.

For this geometry integration in (3) can be approximated using the *Stationary Phase Approximation* (SPA), which method forms the backbone of 2.5D WFS.

The SPA is a method of asymptotic analysis, and provides approximate formula for integrals with a rapidly oscillating kernel. Application of the SPA to the convolution integral (3) was investigated in details recently[6], and the following physical interpretation was established. Physically, the SPA states that the integral providing the radiated field at $\mathbf{x}$ is dominated by those SSD elements $\mathbf{x}_0$, whose sound field in $\mathbf{x}$ propagates into the same direction as the target sound field in $\mathbf{x}_0$. As a consequence, the SPA assigns a unique stationary position $\mathbf{x}_0$ to each receiver position $\mathbf{x}$. On the other hand, each point on the SSD dominates the synthesized sound field towards the direction of local propagation of the target sound field $\mathbf{k}(\mathbf{x}_0)$, measured on the actual SSD element.

Substituting the driving functions into the SFS integral (2) and integrating with respect to time yields the synthesized field inside the enclosure, with $x_0, y_0 \in C$

$$P(\mathbf{x},t,\omega_0) = \frac{\mathrm{j}k_0}{8\pi^2} \oint\limits_C \int_{-\infty}^{\infty} w \frac{R_{\mathrm{n}}\left(\mathbf{x}_0, t - \frac{|\mathbf{x}-\mathbf{x}_0|}{c} - \tau\right)}{\Delta\left(\mathbf{x}_0, t - \frac{|\mathbf{x}-\mathbf{x}_0|}{c} - \tau\right)} \frac{\mathrm{e}^{\mathrm{j}\omega_0\left(t - \frac{|\mathbf{x}-\mathbf{x}_0|}{c} - \tau\left(\mathbf{x}_0, t - \frac{|\mathbf{x}-\mathbf{x}_0|}{c}\right)\right)}}{\Delta\left(\mathbf{x}_0, t - \frac{|\mathbf{x}-\mathbf{x}_0|}{c} - \tau\right)|\mathbf{x}-\mathbf{x}_0|} \mathrm{d}z_0 \mathrm{d}y_0 \mathrm{d}x_0. \quad (22)$$

Integration with respect to z_0 may be approximated applying the SPA[18,19]:

$$\int_{-\infty}^{\infty} F(z) \mathrm{e}^{-\mathrm{j}\phi(z)} \mathrm{d}z \approx \sqrt{\frac{2\pi}{\mathrm{j}|\phi''(z_s)|}} F(z_s) \mathrm{e}^{-\mathrm{j}\phi(z_s)}, \quad (23)$$

where the stationary point z_s is defined as $\frac{\partial}{\partial z}\phi(z)\big|_{z=z_s} = 0$. As both the source and receiver are located at $z = 0$, the trivial stationary point of integral (22) is $z_s = 0$. The phase function under consideration is

$$\phi(z_0) = -\omega_0 \left(t - \frac{|\mathbf{x}-\mathbf{x}_0|}{c} - \tau\left(\mathbf{x}_0, t - \frac{|\mathbf{x}-\mathbf{x}_0|}{c}\right)\right) \quad (24)$$

and its second derivative wrt. z_0 in the stationary point $z_0 = 0$ is given as (for derivation refer to the Appendix)

$$\left.\frac{\partial^2 \phi(z_0)}{\partial z_0^2}\right|_{z_0=0} = k_0 \frac{|\mathbf{x}-\mathbf{x}_0| + \left|\mathbf{x}_0 - \mathbf{x}_s\left(t - \frac{|\mathbf{x}-\mathbf{x}_0|}{c} - \tau\right)\right|}{|\mathbf{x}-\mathbf{x}_0|\Delta\left(\mathbf{x}_0, t - \frac{|\mathbf{x}-\mathbf{x}_0|}{c} - \tau\right)} \quad (25)$$

Denoting the in-plane distances by $r = \mathbf{x} - \mathbf{x}_0$, $R(t) = \mathbf{x}_0 - \mathbf{x}_s(t)$ and substituting back into (22), the synthesized field is approximated as

$$P(\mathbf{x},t,\omega_0) = \oint\limits_C w \frac{R_{\mathrm{n}}\left(\mathbf{x}_0, t - \frac{r}{c} - \tau\right)}{\Delta(\mathbf{x}_0, t - \frac{r}{c} - \tau)} \sqrt{\frac{\mathrm{j}k_0}{2\pi}} \sqrt{\frac{r\Delta(\mathbf{x}_0, t - \frac{r}{c} - \tau)}{r + R(t - \frac{r}{c} - \tau)}} \frac{1}{4\pi} \frac{\mathrm{e}^{\mathrm{j}\omega_0(t - \frac{r}{c} - \tau(\mathbf{x}_0, t - \frac{r}{c}))}}{\Delta(\mathbf{x}_0, t - \frac{r}{c} - \tau) r} \mathrm{d}y_0 \mathrm{d}x_0 \quad (26)$$

Since the time variable is present with a constant temporal shift $t - \frac{r}{c}$ the integral can be reformulated as

$$P(\mathbf{x},t,\omega_0) = \oint\limits_C w \frac{R_{\mathrm{n}}(\mathbf{x}_0, t_0 - \tau)}{\Delta(\mathbf{x}_0, t_0 - \tau)} \sqrt{\frac{\mathrm{j}k_0}{2\pi}} \sqrt{\frac{r\Delta(\mathbf{x}_0, t_0 - \tau)}{r + R(t_0 - \tau)}} \frac{\mathrm{e}^{\mathrm{j}\omega_0(t_0 - \tau(\mathbf{x}_0, t_0))}}{\Delta(\mathbf{x}_0, t_0 - \tau)} \frac{1}{4\pi} \frac{\delta(t - t_0 - \frac{r}{c})}{r} \mathrm{d}t_0 \mathrm{d}y_0 \mathrm{d}x_0. \quad (27)$$

The integral is written in terms of the time-domain Green's function, therefore comparison with (2) yields the final 2.5D driving functions:

$$D_{2.5\mathrm{D}}(\mathbf{x}_0, t_0, \omega_0) = w\sqrt{d_{\mathrm{ref}}(\mathbf{x}_0, t_0)} \sqrt{\frac{\mathrm{j}k_0}{2\pi}} \frac{R_{\mathrm{n}}(t_0 - \tau)}{\Delta(\mathbf{x}_0, t_0 - \tau)} \frac{\mathrm{e}^{\mathrm{j}\omega_0(t_0 - \tau(\mathbf{x}_0, t_0))}}{\Delta(\mathbf{x}_0, t_0 - \tau)}, \quad (28)$$

where the *referencing function* $d_{\mathrm{ref}}(\mathbf{x}_0, t_0)$ is given by

$$d_{\mathrm{ref}}(\mathbf{x}_0, t_0) = \frac{r \cdot \Delta(\mathbf{x}_0, t_0 - \tau)}{r + R(t_0 - \tau)}. \quad (29)$$

In order to get an insight into the structure of the driving function it can be rearranged as

$$D_{2.5\mathrm{D}}(\mathbf{x}_0, t_0, \omega_0) = \underbrace{\sqrt{\frac{2\pi r}{\mathrm{j}k_0}}}_{\substack{\text{SSD}\\ \text{compensation}}} \underbrace{\sqrt{\frac{\Delta(\mathbf{x}_0, t_0 - \tau)}{r + R(t_0 - \tau)}}}_{\substack{\text{virtual source}\\ \text{compensation}}} \underbrace{(-2) w \frac{\partial}{\partial \mathbf{n}_{\mathrm{in}}} P_m(\mathbf{x}_0, t_0, \omega_0)}_{\substack{\text{3D}\\ \text{driving function}}}. \quad (30)$$

The driving function therefore consists of the simple 3D WFS driving functions, adjusted by two correctional factors: the geometry under discussion theoretically would be able to perfectly synthesize a 2D sound field with a set of infinite line sources (described by the 2D Green's function) using a 2D driving function[20]. In the present case, however, 3D point sources (described by the 3D Green's function) are applied to synthesize a 3D sound field. This causes both a secondary source and a virtual source dimensional mismatch.

The secondary source correction factor compensates for the discrepancy between the frequency responses and attenuation factors of the 2D and 3D Green's functions. Obviously, the amplitude factor can be optimized for a fixed distance from each SSD element, given by r.

The virtual source compensation factor resolves the virtual source dimensionality mismatch, correcting the

virtual source attenuation factor. The correction factor gains physical meaning in the stationary SSD point—i.e. where $(\mathbf{x}_0 - \mathbf{x}_s(t_0 - \tau))$ and $(\mathbf{x} - \mathbf{x}_0)$ point in the same direction, thus $|\mathbf{x}_0 - \mathbf{x}_s(t_0 - \tau)| + |\mathbf{x} - \mathbf{x}_0| = |\mathbf{x} - \mathbf{x}_s(t_0 - \tau)| = r + R(t_0 - \tau)$, refer to Figure 3 for the geometry. For the stationary SSD element the numerator corrects the 3D driving function to a ideal 2D one[20] (since the field of a moving infinite line source would attenuate by a factor $\sim 1/\sqrt{\Delta}$), while the denominator adjusts the correct attenuation factor from a 2D moving source to a 3D one using the corresponding static distances—due to the static SSD elements. This statement gives us an important insight into the WFS compensation factors, also reflecting that the vertical and horizontal SPAs are inherently related, since the result of the vertical SPA can be physically interpreted only in the horizontal stationary point.

For an arbitrary source signal, with the frequency content being $Q(\omega_0) = \int_{-\infty}^{\infty} q(t)\mathrm{e}^{-\mathrm{j}\omega_0 t}\mathrm{d}t$ the driving function is written as the weighted sum of the spectral components

$$d_{2.5\mathrm{D}}(\mathbf{x}_0, t_0) = \frac{1}{2\pi}\int_{-\infty}^{\infty} D_{2.5\mathrm{D}}(\mathbf{x}_0, t_0, \omega_0) Q(\omega_0)\mathrm{d}\omega_0 = w\sqrt{d_{\mathrm{ref}}(\mathbf{x}_0, t_0)}\frac{R_{\mathrm{n}}(t_0 - \tau)}{\Delta(\mathbf{x}_0, t_0 - \tau)^2} \frac{1}{2\pi}\int_{-\infty}^{\infty}\sqrt{\frac{\mathrm{j}k_0}{2\pi}} Q(\omega_0)\mathrm{e}^{\mathrm{j}\omega_0(t_0 - \tau(\mathbf{x}_0, t_0))}\mathrm{d}\omega_0. \quad (31)$$

The integral describes an inverse Fourier-transform of the source signal, taken at $t_0 - \tau(\mathbf{x}_0, t_0)$ pre-filtered with a filter, defined by its transfer function $H(\omega_0) = \sqrt{\frac{\mathrm{j}\omega_0}{2\pi c}}$. The driving function in the time domain therefore reads

$$d_{2.5\mathrm{D}}(\mathbf{x}_0, t_0) = w\sqrt{d_{\mathrm{ref}}(\mathbf{x}_0, t_0)}\frac{R_{\mathrm{n}}(t_0 - \tau)}{\Delta(\mathbf{x}_0, t_0 - \tau)} \frac{h(t_0) *_{t_0} q(t_0 - \tau(\mathbf{x}_0, t_0))}{\Delta(\mathbf{x}_0, t_0 - \tau)}, \quad (32)$$

where $h(t_0) = \mathcal{F}_{\omega}^{-1}\left\{H(\frac{\mathrm{j}\omega}{2\pi})\right\}$.

EZEKNEK NINCS MOST HELYK

Integration along the z_0 axis will result in the 2.5D driving functions with a correction term, still depending on the receiver position and frequency. Finally, dependency on the listener position can be eliminated by introducing a properly chosen referencing function. This may be done by further utilizing the SPA concept in order to ensure an amplitude correct synthesis on an arbitrary reference curve. The derivation is explained in details in the corresponding section, applied directly for a moving virtual point source.

It is important to note, that for a linear SSD—as a special SSD curve—the synthesized field is correct within the validity of the SPA, since it is derived from the Rayleigh-integral directly. Any other SSD shape will introduce further errors due to the Kirchhoff/Physical Optics approximation.

C. Defining the referencing function:

The correct choice of the referencing function allows us to optimize the synthesis on an arbitrary shaped reference curve in front of the SSD. According to the SPA each SSD element contributes to the total synthesized field in one unique direction, assigned by the local propagation direction of the virtual sound field, taken on that SSD element. Therefore, the shape of the curve at which the synthesis is optimized can be controlled by adjusting the amplitude of the corresponding stationary SSD elements. This can be formulated mathematically using the normalized wavenumber vector[6], defined by

$$\hat{\mathbf{k}}(\mathbf{x}_0, t) = \frac{\mathbf{k}(\mathbf{x}_0, t)}{k(\mathbf{x}_0, t)} = \frac{\nabla\angle P(\mathbf{x}, t, \omega)|_{\mathbf{x}=\mathbf{x}_0}}{\frac{1}{c}\frac{\partial}{\partial t}\angle P(\mathbf{x}_0, t, \omega)}, \quad (33)$$

where $k(\mathbf{x}, t) = \omega(\mathbf{x}, t)/c$ is the acoustic wavenumber, and the instantaneous frequency is defined as $\omega(\mathbf{x}, t) = \frac{\partial}{\partial t}\angle P(\mathbf{x}, t, \omega)$. In the present case the wavenumber is given as

$$k(\mathbf{x}_0, t) = \frac{1}{c}\frac{\partial}{\partial t_0}\left(\omega_0(t_0 - \tau(\mathbf{x}_0, t_0))\right) = k_0\frac{R(t_0 - \tau)}{\Delta(\mathbf{x}_0, t_0 - \tau)} \quad (34)$$

and the normalized wavenumber vector reads

$$\hat{\mathbf{k}}(\mathbf{x}_0, t) = \frac{\mathbf{x}_0 - \mathbf{x}_s(t_0 - \tau)}{R(t_0 - \tau)}. \quad (35)$$

The distance at which amplitude correct synthesis is ensured is given by the secondary source compensation factor, in a distance r from the stationary SSD element. The locations of amplitude correct synthesis are therefore given as

$$\mathbf{x}_{\mathrm{ref}} = \mathbf{x}_0 + \hat{\mathbf{k}}(\mathbf{x}_0, t)r. \quad (36)$$

and by substituting back (35) and expressing r in terms of d_{ref} from (29)

$$\mathbf{x}_{\mathrm{ref}} = \mathbf{x}_0 + d_{\mathrm{ref}}(\mathbf{x}_0, t_0)\frac{\mathbf{x}_0 - \mathbf{x}_s(t_0 - \tau)}{\Delta(\mathbf{x}_0, t_0 - \tau) - d_{\mathrm{ref}}(\mathbf{x}_0, t - \tau)}. \quad (37)$$

For an illustration on the local wavenumber vector and the explanation of this referencing approach in this dynamic scenario see Figure 3.

As a simple example the synthesis using a linear SSD is considered, with referencing to a straight line parallel with the SSD, termed as *reference line*.

For the given geometry $\mathbf{x}_0 = [x_0,\ y_0 = \text{const},\ 0]$, $\mathbf{n}_{\mathrm{in}} = [0,\ 1,\ 0]^{\mathrm{T}}$, and the reference curve given by $\mathbf{x}_{\mathrm{ref}} = [x_0,\ y_{\mathrm{ref}},\ 0]$, where $y_{\mathrm{ref}} > y_0$. Expressing the referencing function from (37) leads us to

$$d_{\mathrm{ref}}(\mathbf{x}_0, t_0) = \Delta(\mathbf{x}_0, t_0 - \tau)\frac{\mathbf{x}_{\mathrm{ref}} - \mathbf{x}_0}{\mathbf{x}_{\mathrm{ref}} - \mathbf{x}_s(t_0 - \tau)}. \quad (38)$$

Since in the current case the x-coordinates of the reference curve are arbitrary, the referencing function is written purely in terms of the y-coordinates. Along with that, with $R_{\mathrm{n}} = \left\langle\ (\mathbf{x}_0 - \mathbf{x}_s(t)) \cdot [0,\ 1,\ 0]^{\mathrm{T}}\right\rangle = y_0 - y_s(t)$,

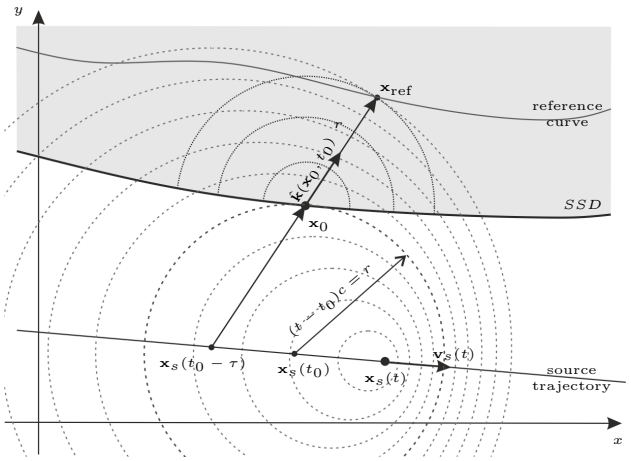

FIG. 3. Illustration of the stationary SSD position including moving source dynamics. The "snapshot" is taken at t. According to the stationary phase approximation the SSD element $\mathbf{x}_0$ determines the synthesized field along the direction, given by the local wavenumber vector $\hat{\mathbf{k}}(\mathbf{x}_0, t_0)$. At the time instant t_0 the wave front of the moving source, arriving to $\mathbf{x}_0$ is described by a spherical wave front, emerging from the virtual source position at $\mathbf{x}_s(t_0-\tau)$, therefore its propagation direction at $\mathbf{x}_0$ is described by $\mathbf{k}(\mathbf{x}_0, t_0) = \mathbf{x}_0 - \mathbf{x}_s(t_0-\tau)$. If an other spherical wave front is generated by the SSD element at $\mathbf{x}_0$, than in any later time instant $t > t_0$ the virtual wavefront and the secondary wavefront coincide along the direction of $\hat{\mathbf{k}}(\mathbf{x}_0, t_0)$. Here $t = \frac{r}{c}$, where r is the distance of the stationary SSD element from the reference curve at which the amplitude correction is optimized. Obviously, by controlling the distance r, the shape of the reference curve can be adjusted according to (37).

and assuming, that the virtual source does not cross the SSD (i.e. $w(\mathbf{x}_0) = 1$) the final driving functions read

$$D_{2.5\mathrm{D}}(\mathbf{x}_0, t_0, \omega_0) = \sqrt{\frac{y_{\mathrm{ref}} - y_0}{y_{\mathrm{ref}} - y_s(t_0-\tau)}} \sqrt{\frac{\mathrm{j}k_0}{2\pi}} \left(y_0 - y_s(t_0-\tau)\right) \frac{\mathrm{e}^{\mathrm{j}\omega_0(t_0-\tau(\mathbf{x}_0,t_0))}}{\Delta(\mathbf{x}_0, t_0-\tau)^{\frac{3}{2}}}. \tag{39}$$

This driving function is the traditional WFS driving function as given by e.g. Verheijen and Start for a stationary virtual point source[2,3], with the original stationary distances replaced with the corresponding dynamic ones. Using this driving function, evaluating the integral along x_0 for the synthesized field by a further application of the SPA would explicitly result in the target sound field[3].

For the special case of a source, moving uniformly at a straight trajectory parallel to the SSD the equation for τ may be solved explicitly. Introducing this solution the present driving function would yield the driving functions, given in [10].

IV. SIMULATION RESULTS:

Two examples are presented in order to demonstrate the validity of the driving functions. All simulations were

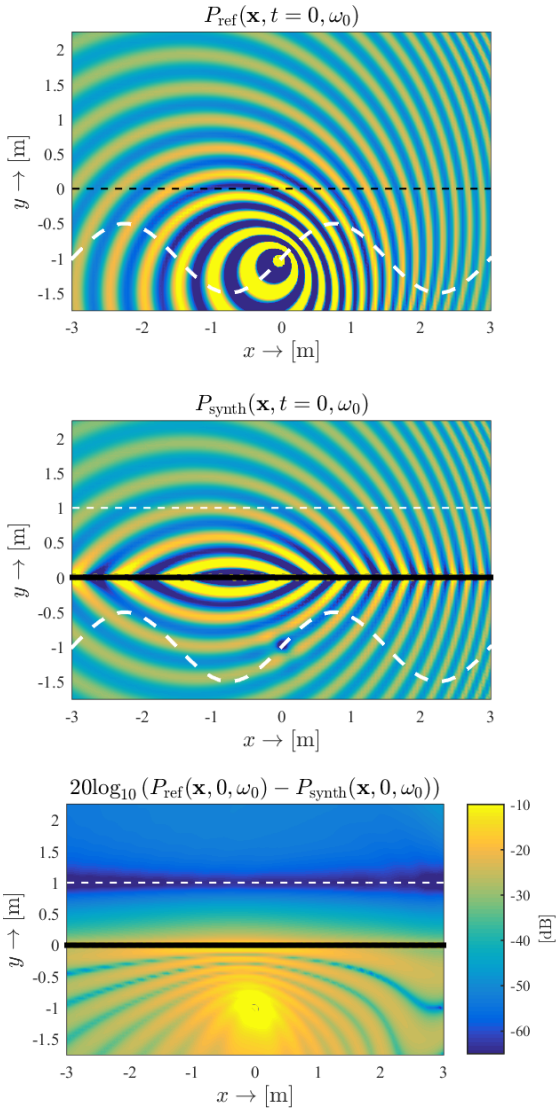

FIG. 4. Synthesis of a point source, moving on a sinusoid trajectory: the spatial distribution of the target sound field (a), the synthesized field (b) and the difference measured in dB scale (c) at $t = 0$.

carried out in the time domain, by evaluating

$$p_{\mathrm{synth}}(\mathbf{x}, t) = \sum_{\mathbf{x}_0} \frac{d\left(\mathbf{x}_0, t - \frac{|\mathbf{x}-\mathbf{x}_0|}{c}\right)}{|\mathbf{x}-\mathbf{x}_0|} \mathrm{d}\mathbf{x}_0, \tag{40}$$

with the sampling weighting factor defined for the actual synthesis geometry[8]. The evaluation requires the solution of the non-linear equation for τ in each field point for each SSD element, resulting in great computational complexity.

A. Synthesis using linear SSD

First, the synthesis with a linear SSD and a reference line is investigated. In this example consider a source, oscillating at $\omega_0 = 2\pi \cdot 1000$ rad/s, and with the trajectory

given by $\mathbf{x}_s(t) = [v_0 t,\ 0.5\sin\left(\frac{2\pi}{\lambda_x} v_0 t\right) - 1,\ 0]^{\mathrm{T}}$, where $v_0 = 150$ m/s and $\lambda_x = 3$ m. The source therefore moves on a sinusoid trajectory, with the time-variant instantaneous speed given by $v(t) = v_0\sqrt{1 + \left(\frac{\pi}{\lambda_x}\right)^2 \cos^2\left(\frac{2\pi}{\lambda_x} v_0 t\right)}$. The SSD is located at $y_0 = 0$. The ideally continuous, infinite SSD was truncated at $|x_0| < 15$ m and sampled at $\Delta x_0 = 0.05$ m. With these parameters the truncation and discretization artifacts are minimal.

The result of synthesis is shown in figure 4 (b) along with the target sound field in (a) at $t = 0$. Similarly to the stationary case, phase correct synthesis can be achieved in the whole listening plane $y > y_0$. As figure 4 (c) confirms—depicting the error between the target and the synthesized field—the synthesis is optimized on the reference line, exhibiting a minimum of the amplitude error along $y = y_{\mathrm{ref}}$.

It should be noted here, that due to the equivalent scattering interpretation of the SFS problem, the error image gives the phase correct solution for the scattering of the same moving source over $y < y_0$ from an infinite plane, located at $y = y_0$, and being approximately amplitude correct along $y = -y_{\mathrm{ref}}$.

B. Synthesis using circular SSD

Although giving an optimal solution within the context of the SPA, with the least approximations introduced, the linear geometry is capable of the reconstruction of sources, only moving behind the SSD. Also the reproduction of the entire motion would require an infinite SSD. Besides, it has been shown recently, that spatial aliasing artifacts— emerging due to the discrete nature of the SSD in real-life applications–are enhanced for the straight SSD case, resulting in unwanted frequency components in the synthesized field[12], which effects are suppressed in case of a smooth enclosing SSD. Therefore, in the aspect of practical applications employment of enclosing SSDs is feasible.

The second example presents a more general scenario: the synthesis a moving source with non-linear trajectory, applying a non-linear enclosing SSD.

The SSD is chosen to be a circular one, with the center located at $\mathbf{x}_c = [-1,\ 1,\ 0]^{\mathrm{T}}$ and the radius of $R_{\mathrm{SSD}} = 2$ m. The virtual source oscillates at $\omega_0 = 2\pi{\cdot}1000$ rad/m, traveling along a exponential trajectory, with its location given by $\mathbf{x}_s = [v_0 t + 1.5, \mathrm{e}^{v_0 t/1.25} - 2.5,\ 0]^{\mathrm{T}}$, where $v_0 = 100$ m/s (the damping factor 1.25 was chosen in order to keep the source speed below the ultrasonic region in the time regime of investigation).

In order to demonstrate, how the synthesis can be optimized on an arbitrary curve, the reference curve was chosen to be a concentric circle inside the SSD with the radius of $R_{\mathrm{ref}} = 1.5$ m. The synthesis was performed by the direct evaluation of (28). In this case the referencing function can be expressed from (37), using that the referencing curve must satisfy equation

$$|\mathbf{x}_{\mathrm{ref}} - \mathbf{x}_c| = R_{\mathrm{ref}}. \tag{41}$$

From the quadratic equation d_{ref} can be expressed explicitly exploiting that $|\mathbf{x}_0 - \mathbf{x}_c| = R_{\mathrm{SSD}}$ and by taking only the real root into consideration.

The time evolution of synthesis is presented in figure 5 in three different time instants. As it can be seen the phase field can be reconstructed perfectly inside the SSD, with the amplitude correct synthesis restricted on the prescribed reference curve: the error distribution has a minimum on the reference circle. Obviously, synthesis is optimized on those parts of the reference curve, for which a stationary SSD element exist, restricting the amplitude correct synthesis to an arc, with its position depending on the virtual source position at the emission time, and the length of the arc depends on the distance of the virtual source measured from the SSD.

Since investigating the spatial characteristics of the synthesis verified that the phase of the virtual sound field can be resynthesized over the whole listening area perfectly, with optimizing the amplitude distribution on an arbitrary receiver curve *at any time instant*, therefore the examination of the temporal characteristics is negligible. The time history of a virtual source pass-by could be synthesized with minimal amplitude error on any point on the reference line in the first example, while in the second example amplitude errors rise on the reference circle when no stationary SSD element can be found for the given listener position due to the actual virtual source position.

V. AN EFFICIENT IMPLEMENTATION SCHEME:

The derivation of the driving functions, presented in the foregoing, assumed that the source position at the emission time instant—and the corresponding propagation delay τ—is known a-priori. The implementation of the driving functions therefore requires the solution of (13) for each SSD element at each time instant, which makes real-time implementation unfeasible.

In order to decrease the computational cost of the implementation a simple finite difference scheme may be applied, by approximating $\tau(\mathbf{x}, t)$ with its first order Taylor's approximation:

$$\tau(\mathbf{x}, t + \mathrm{d}t) = \tau(\mathbf{x}, t) + \mathrm{d}t \frac{\mathrm{d}}{\mathrm{d}t}\tau(\mathbf{x}, t). \tag{42}$$

The temporal derivative of $\tau(\mathbf{x}, t)$ is given by

$$\frac{\mathrm{d}}{\mathrm{d}t}\tau(\mathbf{x}, t) = \tau'(\mathbf{x}, t) = \frac{-\frac{1}{c}\left\langle \mathbf{v}_s(t-\tau)\cdot(\mathbf{x} - \mathbf{x}_s(t-\tau))\right\rangle}{\Delta(\mathbf{x}, t-\tau)}. \tag{43}$$

Therefore after choosing a proper sampling frequency $f_{\mathrm{s}} = 1/\mathrm{d}t$ the discretized form of the field radiated by a moving point source can be calculated at $t = n \cdot \mathrm{d}t$ as

$$p(\mathbf{x}, n) = \frac{1}{4\pi}\frac{q(n\cdot\mathrm{d}t - \tau(\mathbf{x}, n))}{\Delta(n\cdot\mathrm{d}t - \tau(\mathbf{x}, n))}, \tag{44}$$

where

$$\tau(\mathbf{x}, n) = \tau(\mathbf{x}, n-1) + \mathrm{d}t \cdot \tau'(\mathbf{x}, n-1). \tag{45}$$

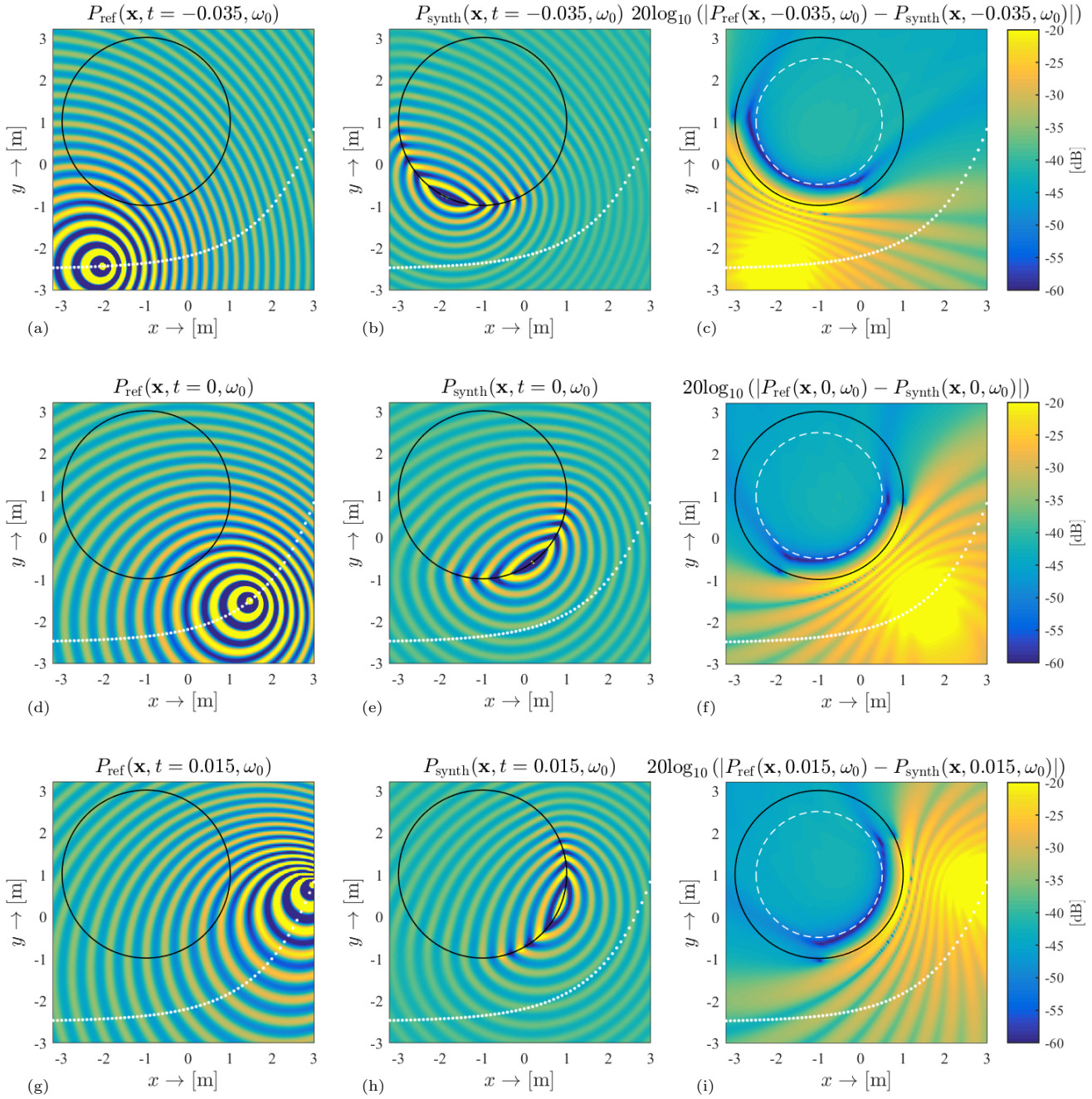

FIG. 5. Time evolution of the synthesis of a moving point source using a circular SSD. The snapshots were taken at $t = -35$ ms (a-c), $t = 0$ ms (d-f) and $t = 15$ ms (g-i). The figures show the real part of the target sound field (a,d,g), the synthesized field (b,e,h) and the absolute error of the synthesis (c,f,i).

Obviously, this approximation requires the solution of (13) for τ at one time instant, e.g. at the time origin. Once it is solved, the field can be calculated iteratively using the above equations. Applying the iterative description makes the real-time implementation of the driving functions possible.

Figure 6 shows the result of the iterative approximation of $\tau(\mathbf{x}, t)$ for the case of a sinusoid trajectory, presented in section IV.A, with all the simulation parameters being the same. The time evolution of $\tau(\mathbf{x}, t)$ is evaluated at $\mathbf{x} = [0, 0, 0]^{\mathrm{T}}$, with the sampling frequency set to $f_{\mathrm{s}} = 10$ kHz. Numerical tests showed a high-stability of the presented solution, with the greatest relative error (≈ 1 %) present around the time origin, where $\tau(\mathbf{x}, t)$ is highly non-linear. This error can be efficiently suppressed by increasing the sampling frequency. Obviously, since all the state-variables are updated from the analytically known source position vector $\mathbf{x}_s(t)$, therefore the perfect tracking of the prescribed trajectory is inherently ensured.

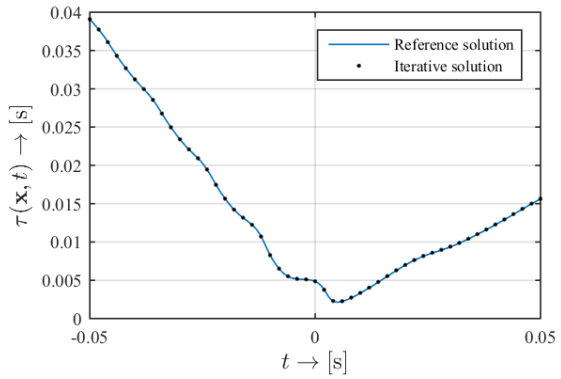

FIG. 6. Comparison of the calculated propagation time delay τ by the direct solution of (13) (solid line), serving as a reference solution, and by approximating with the iterative finite difference scheme given by (45) (dotted line).

The further investigation of the stability and accuracy of this iterative technique falls beyond the scope of the present treatise.

VI. CONCLUSION:

The article presented the general Wave Field Synthesis driving functions for the synthesis of a source, moving on an arbitrary trajectory.

The derivation utilized the unified WFS theory for arbitrary shaped loudspeaker ensemble, stemming from the physical optics approximation of the Kirchhoff-Helmholtz integral. Adapting the theory to the dynamic description of arbitrarily moving point sources, and applying the stationary phase approximation to a properly chosen 3D geometry the 2.5D WFS driving functions were expressed for an arbitrary SSD contour. These driving functions include the referencing function, that's appropriate choice allows to optimize the synthesis to an arbitrary shaped receiver curvature, termed the reference curve. It was shown how the SPA can be interpreted physically by taking the source dynamics into account, achieving a virtual source-stationary secondary source wave front matching both in the spatial and the temporal domain.

The validity of the presented WFS driving functions was demonstrated via pathological examples with a prescribed time-dependent source position function $\mathbf{x}_s(t)$. It was shown, that the amplitude correct synthesis can be controlled perfectly by applying the referencing schemes, that were proposed for stationary virtual sound field[6], with taking the virtual field dynamics into consideration.

In the aspect of practical applicability the a-priory knowledge of $\mathbf{x}_s(t)$ is an optimistic assumption. Instead, more often a parametric curve is given, which the virtual source moves along with a pre-defined velocity profile– e.g. with constant speed—. The derivation of $\mathbf{x}_s(t)$ from the parametric curve and the given velocity profile is not straightforward, it is a frequently emerging problem in the field of e.g. computer graphics and robotics. Analytical solutions are barely available, generally numerical integration is involved in order to estimate the arc length[21]. The further investigation of this topic is however out of the scope of the present article.

The driving functions, presented relied on the a-priori knowledge of the propagation time delay, the time, that acoustic waves need to propagate from the source position at the emission time to the listening position, leading to a non-linear equation. In order to obtain a real-time implementable driving function a finite difference solution was presented, relying on the first order Taylor's approximation of the propagation time delay. By applying this approach the non-linear equation has to be solved only at a single time instant, and the driving functions may be calculated iteratively, making real-time applications of the foregoing possible.

[1] A. J. Berkhout, "Acoustic control by wave field synthesis", The Journal of the Acoustical Society of America **93**, 2764 (1993), URL `http://dx.doi.org/10.1121/1.405852`.

[2] E. Start, "Direct sound enhancement by wave field synthesis", Ph.D. thesis, Delft University of Technology (1997).

[3] E. Verheijen, "Sound reproduction by wave field synthesis", Ph.D. thesis, Delft University of Technology (1997).

[4] S. Spors, R. Rabenstein, and J. Ahrens, "The Theory of Wave Field Synthesis Revisited", in *Proc. of the 124th Audio Eng. Soc. Convention* (Amsterdam) (2008).

[5] F. M. Fazi and P. A. Nelson, "Sound field reproduction as an equivalent acoustical scattering problem", The Journal of the Acoustical Society of America **134**, 3721 (2013), URL `http://dx.doi.org/10.1121/1.4824343`.

[6] G. Firtha, P. Fiala, F. Schultz, and S. Spors, "Improved referencing schemes for 2.5d wave field synthesis driving functions", IEEE Trans. Audio, Speech, Lang. Process. (2016), submitted for peer review.

[7] J. Ahrens and S. Spors, "Reproduction of Moving Virtual Sound Sources with Special Attention to the Doppler Effect", in *Proc. of the 124th Audio Eng. Soc. Convention* (Amsterdam) (2008).

[8] J. Ahrens, *Analytic Methods of Sound Field Synthesis*, 1st edition (Springer Science Business Media, Berlin) (2012), URL `http://dx.doi.org/10.1007/978-3-642-25743-8`.

[9] G. Firtha and P. Fiala, "Sound field synthesis of uniformly moving virtual monopoles", J. Audio Eng. Soc. **63**, 46–53 (2015), URL `http://dx.doi.org/10.17743/jaes.2015.0004`.

[10] G. Firtha and P. Fiala, "Wave field synthesis of moving sources with retarded stationary phase approximation", J. Audio Eng. Soc. **63**, 958–965 (2016), URL `http://dx.doi.org/10.17743/jaes.2015.0078`.

[11] A. Franck, A. Graefe, K. Thomas, and M. Strauss, "Reproduction of Moving Sound Sources by Wave Field Synthesis: An Analysis of Artifacts", in *Proc. of the 32nd Intl. Conf. Audio Eng. Soc.: DSP For Loudspeakers* (Hillerød) (2007).

[12] G. Firtha and P. Fiala, "Investigation of spatial aliasing artifacts of wave field synthesis for the reproduction of moving virtual point sources", in *in 42nd German Annual Conference on Acoustics (DAGA)* (Aachen, Germany) (2016).

[13] F. Schultz and S. Spors, "Comparing approaches to the spherical and planar single layer potentials for interior sound field synthesis", Acta Acustica united with Acustica **100**, 900–911 (2014), URL `http://dx.doi.org/10.3813/aaa.918769`.

[14] S. Spors, "Extension of an analytic secondary source selection criterion for wave field synthesis", in *Audio Engi-*

neering Society Convention 123 (2007), URL `http://www.aes.org/e-lib/browse.cfm?elib=14356`.

[15] P. M. Morse and K. U. Ingard, *Theoretical Acoustics*, 1st edition (McGraw-Hill Book Company, New York, NY) (1968).

[16] A. T. de Hoop, "Fields and waves excited by impulsive point sources in motion—the general 3D time-domain Doppler effect", Wave Motion **43**, 116–122 (2005), URL `http://dx.doi.org/10.1016/j.wavemoti.2005.07.003`.

[17] F. Zotter and S. Spors, "Is sound field control determined at all frequencies? how it is related to numerical acoustics?", in *Proc. of the AES 52nd International Conference* (Guildford, UK) (2013).

[18] N. Bleistein and R. A. Handelsman, *Asymptotic Expansions of Integrals*, 1st edition (Dover Publications) (1975).

[19] N. Bleistein, *Mathematical Methods for Wave Phenomena* (Academic Press) (1984).

[20] F. Volk and H. Fastl, "Wave field synthesis with primary source correction: Theory, simulation results, and comparison to earlier approaches", in *Proc. of the 133th Audio Eng. Soc. Convention* (San Francisco, USA) (2012).

[21] R. Parent, *Computer Animation: Algorithms and Techniques* (Academic Press) (2002).